Environment International 131 (2019) 104961

Contents lists available at ScienceDirect

Environment International

journal homepage: www.elsevier.com/locate/envint

Genomic characterization, kinetics, and pathways of sulfamethazine biodegradation by *Paenarthrobacter* sp. A01

Lijia Cao[a,b,1], Jiayu Zhang[a,b,1], Renxin Zhao[a,b,c], Yu Deng[d], Jie Liu[a], Wenjie Fu[a,b], Yusha Lei[a,b], Tong Zhang[d], Xiaoyan Li[a,c], Bing Li[a,c,*]

[a] Guangdong Provincial Engineering Research Center for Urban Water Recycling and Environmental Safety, Graduate School at Shenzhen, Tsinghua University, Shenzhen, China
[b] School of Environment, Tsinghua University, Beijing, China
[c] Shenzhen Engineering Research Laboratory for Sludge and Food Waste Treatment and Resource Recovery, Graduate School at Shenzhen, Tsinghua University, China
[d] Environmental Biotechnology Laboratory, The University of Hong Kong, Hong Kong, China

ARTICLE INFO

Handling Editor: Yong-Guan Zhu

Keywords:
Sulfamethazine
Biodegradation
Paenarthrobacter
Pathways
sad genes

ABSTRACT

Biodegradation is an important route for the removal of sulfamethazine (SMZ), one of the most commonly used sulfonamide antibiotics, in the environment. However, little information is known about the kinetics, products, and pathways of SMZ biodegradation owing to the complexity of its enzyme-based biotransformation processes. In this study, the SMZ-degrading strain A01 belonging to the genus *Paenarthrobacter* was isolated from SMZ-enriched activated sludge reactors. The bacterial cells were rod-shaped with transient branches 2.50–4.00 μm in length with most forming in a V-shaped arrangement. The genome size of *Paenarthrobacter* sp. A01 had a total length of 4,885,005 bp with a GC content of 63.5%, and it contained 104 contigs and 55 RNAs. The effects of pH, temperature, initial substrate concentration and additional carbon source on the biodegradation of SMZ were investigated. The results indicated that pH 6.0–7.8, 25 °C and the addition of 0.2 g/L sodium acetate favored the biodegradation, whereas a high concentration of SMZ, 500 mg/L, had an inhibitory effect. The biodegradation kinetics with SMZ as the sole carbon source or 0.2 g/L sodium acetate as the co-substrate fit the modified Gompertz model well with a correlation coefficient (R^2) of 0.99. Three biodegradation pathways were proposed involving nine biodegradation products, among which $C_6H_9N_3O_2S$ and $C_{12}H_{12}N_2$ were two novel biodegradation products that have not been reported previously. Approximately 90.7% of SMZ was transformed to 2-amino-4, 6-dimethylpyrimidine. Furthermore, *sad* genes responsible for catabolizing sulfonamides were characterized in A01 with high similarities of 96.0%–100.0%. This study will fill the knowledge gap in the biodegradation of this ubiquitous micropollutant in the aquatic environment.

1. Introduction

Antibiotics have been recently recognized as an emerging threat to organisms and human health owing to their toxicity and persistence in the environment through a complex vicious cycle of transformation and bioaccumulation (Carvalho and Santos, 2016; Liu et al., 2017; Li et al., 2018). The diffusion of antibiotics in the environment, particularly in aquatic systems, contributes to the development and transmission of antibiotic resistance in environmental pathogens (Deng et al., 2016). This phenomenon has been identified as a global challenge to human health security in the 21st century.

Sulfonamides (SAs) have been intensively used as anti-infectives, particularly in human and veterinary medicine, and are still widely prescribed today (Baran et al., 2011; Majewsky et al., 2015). Sulfamethazine (SMZ), one of the most commonly used SAs (Biošić et al., 2017), is frequently detected in soils (Garcia-Galan et al., 2013), wastewater treatment plants (Li et al., 2013), surface water (Iglesias et al., 2013), groundwater (Spielmeyer et al., 2017) and even drinking water (S. Wang et al., 2015; L. Wang et al., 2015). The reported residual concentrations are in the ng/L to μg/L range, which has been found to pose chronic toxicity to human body and then cause organ lesions. Moreover, long-term exposure leads to resistance in intestinal microorganisms, consequently, antibiotic resistant genes can be conjugated to pathogens through horizontal gene transfer (Liu et al., 2017).

* Corresponding author at: Guangdong Provincial Engineering Research Center for Urban Water Recycling and Environmental Safety, Graduate School at Shenzhen, Tsinghua University, University Town, Shenzhen 518055, China.
E-mail address: bingli@sz.tsinghua.edu.cn (B. Li).
[1] Contributed equally to this work.

https://doi.org/10.1016/j.envint.2019.104961
Received 13 February 2019; Received in revised form 2 June 2019; Accepted 22 June 2019
Available online 19 July 2019

The biological treatment process is an important method for removing SMZ in water bodies (Yin et al., 2014), while on the other hand, it creates an environment potentially suitable for resistance development and spreading, because bacteria are continuously exposed to SMZ residue (Michael et al., 2013). Therefore, it is necessary to understand the biodegradation mechanism of SMZ in biological treatment processes. The majority of studies in this field have focused on the occurrence and distribution of SMZ in the environment (Garcia-Galan et al., 2013; Li et al., 2013) and the removal behaviors by different treatment technologies, particularly advanced oxidation processes (Cheng et al., 2018; Fukahori et al., 2018). However, researches on the biodegradation of SMZ by pure cultures or microbial communities are limited. Several SMZ-degrading strains have been isolated from activated sludge and wastewater. For example, a *Geobacillus* strain S-07 isolated from activated sludge of an antibiotics pharmaceutical factory was able to degrade SMZ at 70 °C (Pan et al., 2017). An *Achromobacter* sp. S-3 with the ability to remove SMZ was isolated from an aerobic sequence batch reactor (Huang et al., 2012). A sulfamethoxazole (SMX)-degrading *Achromobacter denitrificans* strain PR1 that could also degrade SMZ was isolated from activated sludge (Reis et al., 2014). These isolated and characterized microorganisms are able to use SMZ as the sole carbon source and may even dominate in SMZ-degrading systems, indicating the potential application of these microorganisms to eliminate SMZ in real wastewater. Yang et al. (2016) revealed that *Acinetobacter* and *Pseudomonas* represented major bacterial communities involved in SAs degradation in activated sludge. Zhao et al. (2019) reported that an enriched SMZ-degrading bioreactor was composed mainly of *Aridibacter*, *Arthrobacter*, *Geothrix*, *Ferruginibacter*, *Plasticicumulans*, and *Terrimonas*. S. Wang et al. (2015) and L. Wang et al. (2015) found that *Achromobacter* and *Pseudomonas* played dominant roles in the anodic chambers of microbial fuel cell reactors for SMX degradation.

Aside from these studies, little information is known about the kinetics, products, and pathways of SMZ biodegradation owing to the complexity of enzyme-based biotransformation processes. Deng et al. (2016) proposed possible degradation products and pathways of sulfadiazine by two strains belonging to *Arthrobacter*, but no solid evidence was obtained concerning the enzymes responsible for the degradation of SAs to confirm these speculations. Recently, two monooxygenases (SadA and SadB) and one FMN-reductase (SadC) were found in *Microbacterium* sp. strain BR1 to initiate the catabolism of SAs by hydroxylating the sulfonamide molecule at the sulfonyl group (Ricken et al., 2017). This finding provides new insight into the biodegradation mechanisms at the molecular level. To explore related functional genes, genomic sequencing has been conducted to obtain whole genome sequences. However, research on the genomic characterization of these SAs-degrading pure cultures has been conducted sporadically. Thus far, only the genomes of *Arthrobacter* sp. D2 and D4 (Deng et al., 2016), *Microbacterium* sp. BR1 and C448 (Martin-Laurent et al., 2014), *Achromobacter denitrificans* PR1 (Reis et al., 2017) have been sequenced. The genomic sequences of SMZ-degrading isolates are not available on public databases such as the National Center for Biotechnology Information (NCBI), which prevents comparative analysis on a genomic basis for SAs biodegradation.

Considering the aforementioned research gaps, the objectives of this study are to: (i) isolate a high efficiency SMZ-degrading strain and to characterize it based on both morphological and molecular aspects; (ii) investigate the effects of pH, temperature, initial substrate concentration and additional carbon source on the biodegradation of SMZ; (iii) evaluate the variation in biodegradation kinetics under different conditions; and (iv) elucidate comprehensive pathways with combination of detected biodegradation products and related functional genes.

2. Materials and methods

2.1. Chemicals

SMZ (purity 99%) and 2-[N-(4-aminophenyl) amino]-4, 6-dimethylpyrimidine were purchased from Sigma-Aldrich (USA). 2-Amino-4, 6-dimethylpyrimidine (purity 98%) was obtained from Aladdin (China). Acetonitrile and methanol (LC grade) were obtained from Merck KGaA (Germany), and formic acid (LC–MS grade, purity 98%) was purchased from Fluka (Switzerland). Ultrapure water was produced using a Millipore Milli-Q system (Bedford, MA, USA).

2.2. Culture enrichment, isolation and identification

The SMZ-degrading consortia were enriched for five months using 50 mL of activated sludge as the inoculum, which was collected from a local wastewater treatment plant. The bioreactors were set up in parallel with a working volume of 500 mL at room temperature (25 ± 2 °C) and were continuously stirred at 200 rpm for aeration and mixing. The concentrations of mixed liquor suspended solids were maintained at about 1000 mg/L. The initial SMZ concentration in the synthetic wastewater was 20 mg/L and then gradually increased to 150 mg/L according to the removal behaviors. The enriched cultures were serially diluted and were plated on a mineral salt medium (MSM) with 100 mg/L SMZ as the sole carbon source (MSM–SMZ). After 5 days of incubation at 25 °C, 35 single colonies were isolated and individually transferred for further purification. To examine the SMZ degrading capacity, 35 pure cultures were inoculated into liquid MSM–SMZ at 25 °C on an incubator shaker at 150 rpm. Finally, an isolate achieving the highest degrading efficiency was designated as A01, and was preserved at −80 °C in a mixture of 40% glycerol and LB medium for subsequent experiments.

To characterize the microbial community structure of the enriched consortia, PCR amplification of 16S rRNA genes was conducted using the primers F515 (5′-GTGCCAGCMGCCGCGGTAA-3′) and R806 (5′-GGACTACVSGGGTATCTAAT-3′). The 50 μL PCR reaction mixture contained 25 μL of 2 × Premix Taq™ (TaKaRa, Japan), 22 μL of nuclease-free water, 2 μL of forward and reverse primers and 1 μL of sample DNA. The PCR was performed as follows: initial denaturation at 95 °C for 5 min, 28 cycles including 95 °C for 0.5 min, 55 °C for 0.5 min and 72 °C for 1 min, and a final extension step at 72 °C for 5 min (Zhang et al., 2018). The PCR products were purified using the UltraClean PCR clean-up kit (Mo Bio Laboratories, Inc., Carlsbad, CA, USA) and then quantified using NanoDrop spectrophotometer (ND-One, Thermo Fisher Scientific, USA). A single composite sample containing equimolar amounts of barcoded PCR products was produced to obtain equivalent sequencing depth for all samples (Kozich et al., 2013). The sample was sequenced by Novogene (Tianjin, China) on an Illumina MiSeq platform with 250 bp paired-end strategy. All of the raw sequencing data of the 16S rRNA amplicons were processed following the standard pipeline in Mothur (version 1.39.5), including demultiplex, quality trim, alignment, and a final check with chimera.uchime to remove chimeric sequences. Then, the clean sequences were normalized by randomly extracting 18,224 clean sequences, which is the lowest sequencing depth after previous treatment steps from each sample dataset, and were submitted to the Ribosomal Database Project (RDP) Classifier (version 2.11) for taxonomy annotation at an 80% threshold (Wang et al., 2007; Zhang et al., 2018). To identify the taxon of the 35 isolates, genomic DNA was extracted using the FastDNA™ SPIN Kit for Soil (MP Bio, USA). 16S rRNA genes were amplified using primers 27F (5′-AGAGTTTGATCMTGGCTCAG-3′) and 1492R (5′-TACGGYTACCTTGTTACGACTT-3′). The PCR solutions were the same as that mentioned previously. The PCR procedure was performed as follows: initial denaturation at 95 °C for 5 min, 28 cycles including 95 °C for 0.5 min, 55 °C for 0.5 min and 72 °C for 2 min, finally, 72 °C for 8 min. The PCR products were conducted using Sanger sequencing by BGI (Shenzhen, China), and the generated data were annotated via the NCBI 16S ribosomal RNA sequences database. The phylogenesis was analyzed using Molecular Evolutionary Genetics Analysis (MEGA) software (version 7.0.26), and the phylogenetic tree was constructed using neighbor-joining method. MEGA is an integrated tool for conducting automatic and manual sequence alignment, inferring evolutionary trees, estimating genetic distances and diversities (Kumar et al., 2018).

2.3. Morphology characterization

The morphology was observed using scanning electron microscopy (SEM; ZEISS SUPRA® 55, Carl Zeiss, Germany). Isolated strain A01 was inoculated into the MSM–SMZ for 36 h of incubation until the mid-log phase, and was then collected by centrifugation (3000 rpm, 3 min) and washed three times with PBS (50 mM, pH 7.0). Afterward, the cells were fixed with 2.5% glutaraldehyde in PBS at 4 °C overnight. After rinsing with PBS three times, the fixed cells were dehydrated with an ascending series of ethanol solutions at 20%, 50%, 80%, and 100% for 10 min and were then freeze-dried for 48 h in a silicon wafer. The sample was sputter-coated with about 10 nm of platinum before observation and was then operated at 2 kV accelerating voltage.

2.4. Genome sequencing and bioinformatics analysis

The genomic DNA of A01 was sent to Novogene for sequencing on an Illumina Novaseq 6000 platform with 150 bp paired-end strategy, and approximately 2.7 GB of clean data were generated. The de novo assembly for the sequences was conducted using Megahit (version 1.0.3) (Li et al., 2016) with the minimum and maximum k-mer size of 21 and 147 respectively, a step of 8, and a minimum contig length of 500 bp. Open reading frames (ORFs) prediction was conducted by Prodigal (version 2.6.3) (Hyatt et al., 2010) and the predicted genes were annotated by the Rapid Annotations using Subsystems Technology (RAST) server (Aziz et al., 2008). To identify the SMZ degrading genes, the BLAST was used to compare the predicted ORFs against the NCBI non-redundant protein (NR) database with a cut-off e-value of 10^{-5}. CheckM (version 1.0.11) was used to assess the completeness and contamination of the genome and extract marker genes of closely related reference genomes retrieved from NCBI (Parks et al., 2015). Genome phylogenetic analysis used CLUSTALW for multiple sequence alignment and MEGA for tree construction. The average nucleotide identity (ANI) values were calculated by OrthoANI (Lee et al., 2016) algorithm to assess the genome-sequence-based similarity among A01 and other reference strains. The GC content was calculated from the genomic sequences. Comparisons of genomes of A01 and other reference strains were conducted by BRIG (version 0.95) (Alikhan et al., 2011). The predicted ORFs were mapped to the Kyoto Encyclopedia of Genes and Genomes (KEGG) database using the BLAST with a cut-off of 10^{-5} for the e-value to find the potential SMZ metabolic pathways (Sangwan et al., 2014).

2.5. Biodegradation experiments

The SMZ biodegradation experiments were performed in 250 mL flasks containing 100 mL MSM–SMZ. The composition of MSM per liter of ultrapure water included 6.81 g of Na_2HPO_4, 0.675 g of KH_2PO_4, 0.112 g of $MgSO_4{\cdot}H_2O$, 0.015 g of $CaCl_2$, and 20.4 mg of NH_4Cl as well as trace elements (Deng et al., 2016). All experiments were conducted in triplicate in the dark at 25 °C using an incubator shaker at 150 rpm.

Growing cells were used to determine the reduction of SMZ concentration and total organic carbon (TOC). Resting cells were used to identify the biodegradation products in 100 mL of PBS (50 mM, pH = 7.0) with 100 mg/L SMZ (PBS–SMZ). To obtain the growing and resting cells, strain A01 was inoculated into the MSM–SMZ and was cultivated until the mid-log phase. The cells were then harvested by centrifugation at 4000 rpm for 5 min and were washed three times with PBS. Finally, the centrifugation pellets were re-suspended in the MSM–SMZ for growing cells and in the PBS–SMZ for resting cells, respectively.

2.6. Analytical methods

2.6.1. SMZ mineralization

The SMZ mineralization was determined by testing the TOC using TOC-L (SHIMADZU, Japan). The samples were diluted with ultrapure water and were filtered by a 0.45 μm PES syringe filter (BOJIN, Germany) prior to measurement.

2.6.2. Bacterial growth

Bacterial growth was determined by measuring the bacteria number using flow cytometry (BD FACSCalibur system, BD Biosciences, CA, USA). The samples were stained by SYBR Green I with a final concentration of 10 μL/mL (Invitrogen, USA), and were incubated in darkness for 15 min at room temperature prior to measurement. The data were analyzed using the BD CellQuest Pro software (BD Biosciences).

2.6.3. SMZ quantification by HPLC–MS/MS

The SMZ was quantified using a high performance liquid chromatography system (HPLC, 20A, SHIMADZU, Japan) equipped with a triple-quadrupole mass spectrometer (MS/MS API 3200, Applied Biosystems/SCIEX, USA) operating with a C18 column (Agilent, 2.1 × 100 mm, 2.7 μm). The MS/MS was performed in positive ionization (ESI+) and multiple reaction monitoring (MRM) mode. Mobile phases A and B were fixed as ultrapure water and acetonitrile respectively with additional 0.1% formic acid (*v*/v) at a flow rate of 0.2 mL/min. The column temperature was 35 °C. The initial mobile phase proportion was 90% (A):10% (B), then A was linearly decreased to 0% within 3 min and was held for 1 min to clean the column using 100% organic mobile phase B. Afterward, A was increased to the initial proportion of 90% in 0.5 min and was kept for 4 min to equilibrate the column before the next injection. The total run time was 8.5 min. The optimal parameters of MS/MS included declustering potential of 30 V, entrance potential of 10 V, collision energy of 26 V, and collision cell exit potential of 2.5 V. The samples were diluted with ultrapure water and were filtered by a 0.22 μm PTFE syringe filter (ANPEL, Shanghai) before measurement. Analyst software (version 1.6.2) was used to collect and analyze the data.

2.6.4. Identification of biodegradation products

Product identification was conducted by HPLC–MS/MS performed in ESI+ and full scan mode (*m/z* 50–500) under the same operating conditions as those mentioned previously. The initial mobile phase proportion was 90% (A):10% (B), then A was linearly decreased to 0% within 13 min and was held for 2 min. Afterward, A was increased to 90% within 1 min and was kept for 4 min. The total run time was 20 min. Each suspected ion was extracted and was further analyzed via daughter ion scan to determine the proposed structures of plausible biodegradation products. The fragment with the highest signal intensity was identified as the primary daughter ion for the corresponding peak. Only peaks appearing in samples after the SMZ biodegradation with a signal intensity three times higher than the background was considered as the a possible *m/z* of the biodegradation product. For further confirmation of the proposed metabolites, standards were purchased and analyzed to check whether the retention time (RT) and fragments were identical to the corresponding biodegradation products.

3. Results and discussion

3.1. Culture enrichment, isolation, and identification

During the enrichment process of the SMZ-degrading consortia, the SMZ concentration was artificially increased when obvious reduction was observed according to the HPLC–MS/MS detection results. After five months of enrichment, the SMZ with a concentration of 150 mg/L could be completely removed within 48 h. The 16S rRNA gene sequences revealed that the microbial communities were composed of six dominant genera: *Aridibacter*, *Paenarthrobacter*, *Geothrix*, *Ferruginibacter*, *Plasticicumulans*, and *Terrimonas*. It is worth mentioning that the genus *Paenarthrobacter* had the highest relative abundance of 16.8% in the enriched consortia (Fig. S1).

In total, 35 pure cultures belonging to 11 genera of 5 phyla were isolated from the enriched consortia (Fig. S2). After incubation in the MSM–SMZ for seven days, isolates were screened according to their prominent removal efficiency of SMZ, and A01 was selected as the experimental strain in this study owing to its highest degradation rate of 100% (Fig. S3). Based on the BLAST results of the nearly full-length 16S rRNA gene against the NCBI 16S ribosomal RNA sequences database, A01 was found to be closely related to *Paenarthrobacter ureafaciens* with similarity of 99% (Fig. S4). Hence, strain A01 was annotated as *Paenarthrobacter* sp. in this study.

3.2. Morphologic and genomic characterization

The SEM image of A01 showed rod-shaped cells in an exponential phase with transient branches 2.50–4.00 μm, most of which forming a V-shaped arrangement (Fig. 1a). The genome size of A01 had a total length of 4,885,005 bp and contained 104 contigs, 55 RNAs, and a GC content of 63.5%. The completeness and contamination of the draft genome were 99.7% and 1.36%, respectively. Moreover, there were 4849 ORFs predicted by Prodigal, 40.2% of which was functionally annotated by the RAST server. The genome harbored 33 proteins involved in stress responses to osmotic pressure, carbon starvation, oxygen radicals, and toxic chemicals. *Paenarthrobacter* has been reported to evolve self-protective mechanisms for survival and prosperity in a variety of stressful environments. Previous studies have revealed that this genus is able to degrade nicotine, atrazine, L-proline and iprodione (Boiangiu et al., 2018; Deutch, 2018; Deutch et al., 2018; Yang et al., 2018). The features in the subsystems also indicate that *Paenarthrobacter* sp. A01 is able to metabolize alkanesulfonate, quinate, benzoate and p-hydroxybenzoate.

Considering that *Paenarthrobacter* is a newly-created genus that includes several species previously belonging to the genus *Arthrobacter* (Busse, 2016), phylogenetic evaluation of A01 was conducted incorporating all eight strains of the genera *Arthrobacter* and *Paenarthrobacter*, the genomes of which are publicly available in the NCBI. As shown in Fig. 1b, the phylogenetic tree placed A01 with *Arthrobacter* sp. D2 as a monophyletic sister group to the group of *Arthrobacter* sp. ATCC 21022 and *Arthrobacter* sp. D4, which means these strains are most closely related. Fig. 1c reveals the ANI values between A01 and the other eight stains of the genus *Arthrobacter* and *Paenarthrobacter*. In agreement with the results of a neighbor joining tree, the high ANI value of 98.78–99.98% between A01 and D2, D4, and ATCC 21022 indicates that they are grouped into the same species (Varghese et al., 2015). The peptidoglycan type of *Paenarthrobacter* is A3α, and the quinone system predominantly contains menaquinone MK-9(H_2), which distinguishes it from *Arthrobacter*. We aligned the 16S rRNA gene sequences of *Arthrobacter* sp. D2, D4 and ATCC 21022 with the updated 16S ribosomal RNA sequences database in the NCBI, and found that these three strains are now reclassified into the genus *Paenarthrobacter*. Hence, it is reasonable that these strains share high similarities. The BRIG plot shows BLAST comparisons of eight reference genomes against the draft genome of A01 (Fig. 1d). For A01 and three previously annotated as *Arthrobacter* strains D2, D4 and ATCC 21022, a few genomic regions of difference were observed. A01 and all of the *Paenarthrobacter* strains including 25_8, Hce-1, TC1, 26Cvi1.1E, and 231Sha2.1M6 were organized with significant pockets of differences concentrated in specific genomic regions.

To further characterize the genomic information of A01 and to elucidate the SMZ metabolic pathway, we focused mainly on the nitrogen and sulfur metabolism of A01, because SMZ might provide a

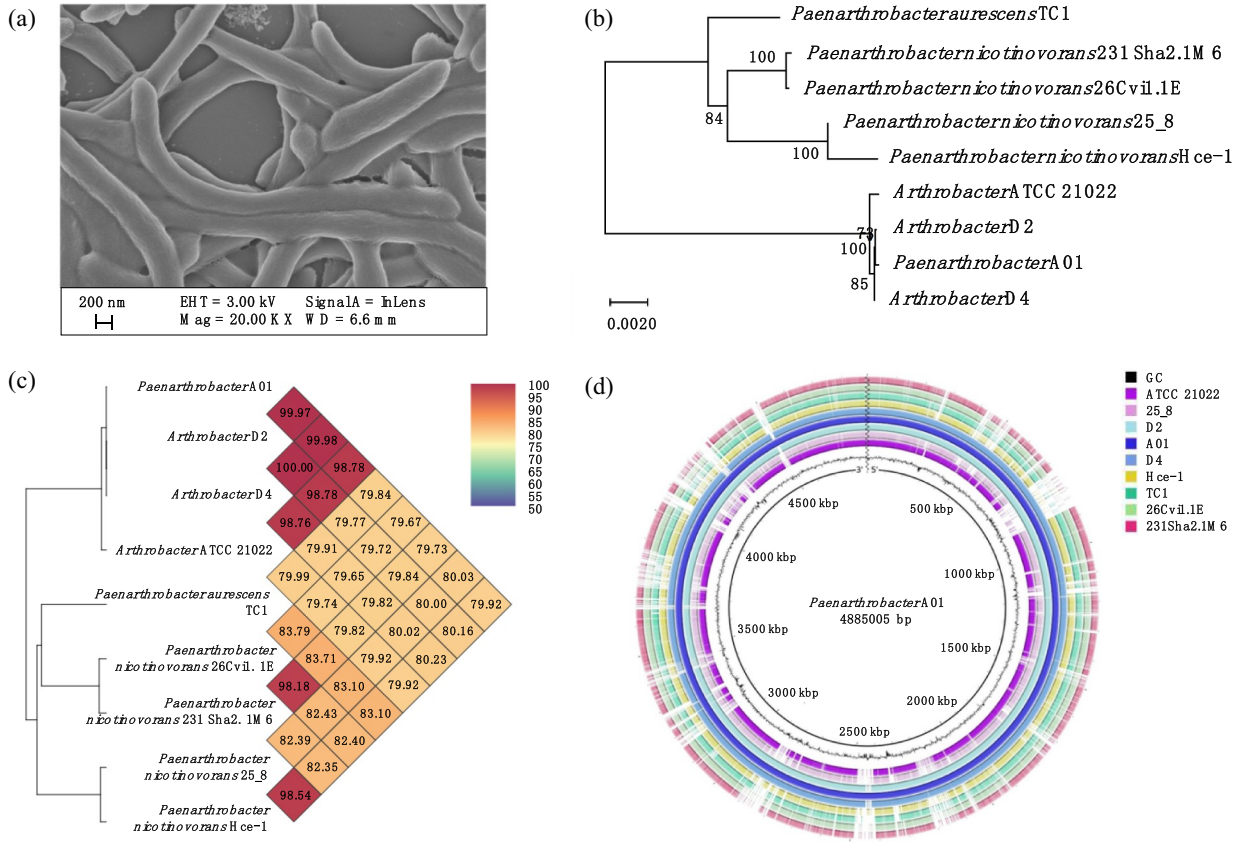

Fig. 1. Morphologic and genomic characterization of *Paenarthrobacter* sp. A01. (a) SEM image. (b) Genome-based phylogenetic tree constructed using concatenated essential proteins. (c) OrthoANI values between *Paenarthrobacter* sp. A01 and other reference strains. (d) Comparative genomic characterization of *Paenarthrobacter* sp. A01. Rings from inside to outside: ring 1, GC skew; rings 2–9, nucleotide alignment with reference strains ATCC 21022, 25_8, D2, A01, D4, Hce-1, TC1, 26Cvi1.1E, and 231Sha2.1M6, respectively.

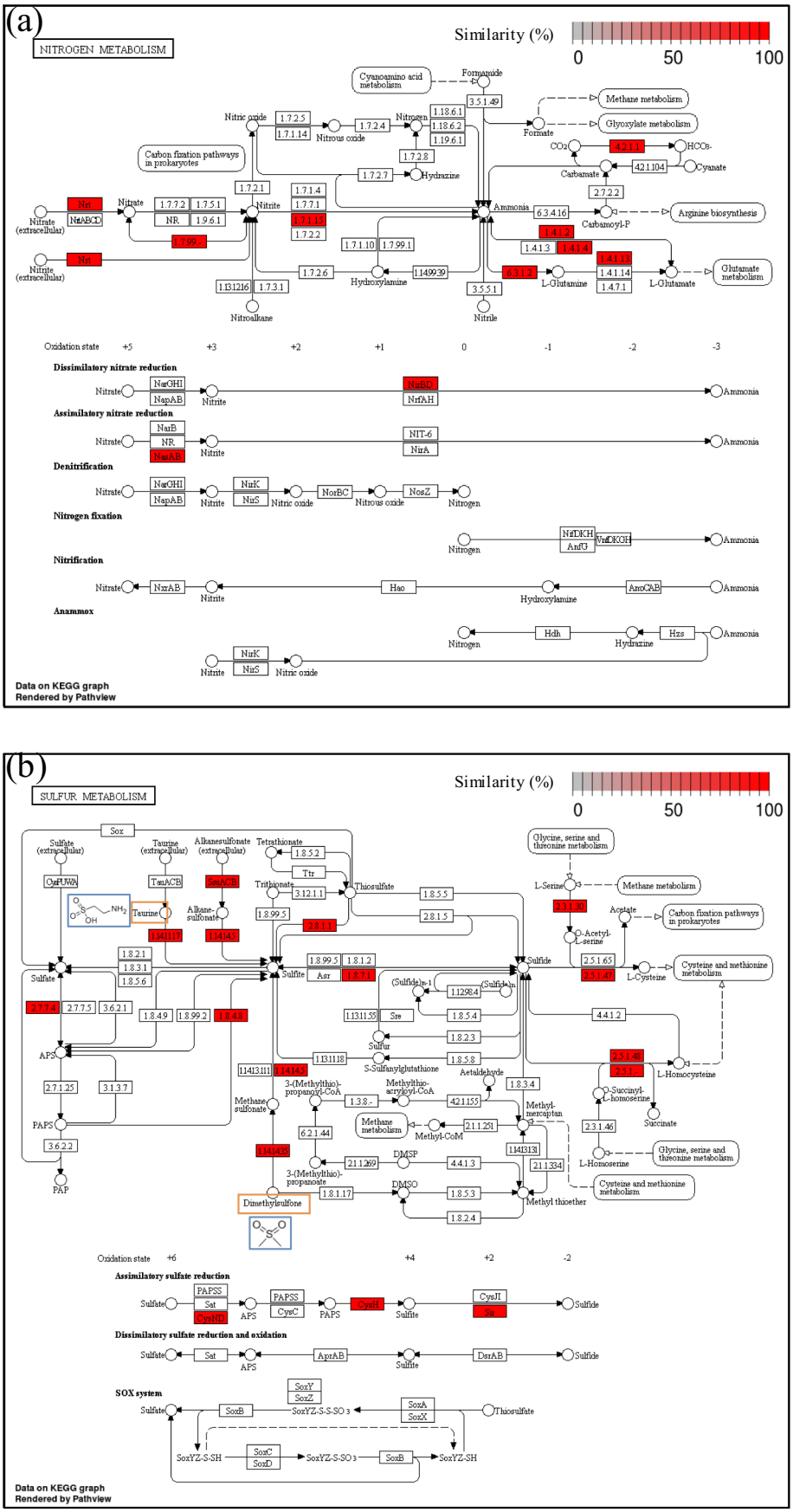

Fig. 2. (a) Nitrogen, and (b) sulfur metabolic pathways of *Paenarthrobacter* sp. A01 obtained from the KEGG database. Red highlighted boxes indicate the existence of functional enzymes involved in the metabolism. (For interpretation of the references to colour in this figure legend, the reader is referred to the web version of this article.)

source of nitrogen and sulfur which are essential for microbial growth. The KEGG database is the most comprehensive and widely used database on metabolic pathways and can build metabolic maps based on the Enzyme Classification (EC) numbers. The nitrogen sources in the medium were NH_4Cl and SMZ, and the existing forms were ammonia, amine and N-containing heterocycles. A01 can utilize glutamine synthetase (EC 6.3.1.2) to convert ammonia into L-Glutamine, which is further transformed to L-Glutamate by glutamate synthase (EC 1.4.1.13). Alternatively, A01 can directly utilize ammonia to synthetize L-Glutamate by glutamate dehydrogenase (EC 1.4.1.2 or EC 1.4.1.4) (Fig. 2a). However, knowledge of the metabolic pathways of amine and the hexahydroxy N-containing heterocyclic compound is limited, and related information is not available in KEGG. The mechanism for utilization of such nitrogen types from SMZ by A01 needs further exploration in the future. The sulfur metabolism map indicates that A01 could not assimilate sulfate owing to the absence of key enzymes such as PAPSS and CysC, which suggests that SMZ is the only available sulfur source (Fig. 2b). Dimethylsulfone sharing the same moiety of -SO_2- with SMZ can be transferred into sulfite by dimethylsulfone monooxygenase (EC 1.14.1435) and alkanesulfonate monooxygenase (EC 1.14.145), followed by an assimilation reaction initiated by assimilatory sulfite reductase (EC 1.8.7.1). Sulfide can subsequently be utilized to synthetize amino acid (L-Cysteine and L-Homocysteine), succinate and acetate to maintain life activities. Taurine is also similar to SMZ in structure partially, it can be transformed to sulfite by taurine dioxygenase (EC 1.14.1117), followed the same reactions as described for dimethylsulfone. These findings suggested that SMZ could follow the same sulfur metabolic pathway as dimethylsulfone and taurine owing to their shared moiety of -SO_2-.

3.3. Biodegradation of SMZ by Paenarthrobacter sp. A01

3.3.1. Effect of pH on SMZ biodegradation

SMZ biodegradation by *Paenarthrobacter* sp. A01 was investigated at pH 6.0, 7.0, and 7.8 (Fig. 3a), an initial SMZ concentration of 100 mg/L and an incubation temperature of 25 °C. In the control group without cells inoculation, no significant removal of SMZ was observed, indicating that volatilization, hydrolysis, or photolytic degradation did not occur under the tested conditions. In the experimental group, SMZ was almost completely removed by A01 in 96 h, and the TOC was reduced by 44.0–45.5%. The biodegradation rate and mineralization rate (Fig. S5a) were negligibly affected by the initial pH, indicating that this pH range (6.0–7.8) is suitable for SMZ biodegradation. This result is also consistent with the bacteria growth trend (Fig. S6a), which showed little differences among the three conditions. It should be noted that the pH remained constant during the entire biodegradation process. Microorganisms originating from different environments have different optimal living conditions and can adapt to contaminants through self-regulation. The degradation of SMX by an *Acinetobacter* sp. strain isolated from activated sludge was significantly inhibited in the acidic condition (pH 5.0) and was slightly influenced in the alkaline condition (pH 9.0) (Wang and Wang, 2017). In contrast, Mao et al. (2018) reported that the SMX removal efficiency declined significantly at pH 7.0–8.0 when degraded by *S. oneidensis* MR-1 and *Shewanella* sp. strain MR-4. Other studies also found that neutral and slightly acidic pH values are more favorable for biodegradation of SMZ (Huang et al., 2012; Pan et al., 2017). One of the possible reasons for the pH effect is that pH variation could change the cell membrane permeability and the activity of proteins and enzymes related to nutrient absorption, and can therefore affect the growth of microorganisms (Zarfl et al., 2008).

3.3.2. Effect of temperature on SMZ biodegradation

Temperature has a strong impact on microbial activity, with optimal temperatures shown for specific microorganisms. For example, the most suitable temperature for thermophile-*Geobacillus* sp. S-07 to degrade SMZ is 70 °C (Pan et al., 2017), whereas that for *Achromobacter* sp. S-3 is 30 °C (Huang et al., 2012). The effect of temperature on SMZ biodegradation by *Paenarthrobacter* sp. A01 is shown in Fig. 3b. At an SMZ concentration of 100 mg/L and pH 7.8, the most rapid degradation and mineralization rates were found at 25 °C. When the temperature decreased to 15 °C, no reduction in SMZ and biomass growth (Fig. S6b) were observed until 72 h. Low temperature retards the combination of enzymes and substrates and thus slows the bacterial growth (Jagdale and Gordon, 1997; Tibbett et al., 1998). When the temperature increased to 35 °C, the SMZ concentration declined gradually after an initial lag phase of 32 h, and the final removal efficiency was only 56.2%. Regarding the comparison of the bacteria growth trend, the final cell concentration at 35 °C accounted for approximately one-third of that at 25 °C. It is widely accepted that each enzyme has an optimal temperature range that varies greatly among microorganisms. Although 35 °C will not lead to protein denaturation, the results showed that this temperature is not suitable for *Paenarthrobacter* sp. A01 growth. The discrepancy in the TOC mineralization rate at different temperatures (Fig. S5b) suggests the effect of temperature on the enzymes involved in the transformation of SMZ and the corresponding biodegradation products (Wang et al., 2018). The effect of temperature on the enzyme activity is reflected mainly in the expression of relevant genes (Wang and Wang, 2018). Wu et al. (2013) found that the abundance of the ammonia monooxygenase gene, which plays an important role in degrading organic pollutants, was lower at 4 °C than at 25 °C. Gui et al. (2017) also reported that temperature influences the expression of denitrifying genes, and thus affects organic pollutant removal.

3.3.3. Effect of initial substrate concentration on SMZ biodegradation

The effect of initial substrate concentration on SMZ biodegradation at 25 °C and pH 7.8 is shown in Fig. 3c. The final biodegradation efficiencies reached to 70.7%, 96.7%, and 95.3% when the initial SMZ concentrations were 10 mg/L, 100 mg/L, and 500 mg/L, respectively. Previous studies have indicated that the biodegradation rate decreases as the concentration of SAs declines, which is possibly attributed to the low bioavailability of the substrate when its concentration is too low (Jiang et al., 2014; Wang et al., 2018). Moreover, if the concentration increases to 500 mg/L, the biodegradation is inhibited with the lag phase extending to 72 h. Afterward, the concentration of SMZ decreases significantly with a rapid increase in the biomass (Fig. S6c). The toxicity of SMZ at high concentration, as well as the accumulation of intermediate products during the degradation process, may result in adverse effects on the microorganisms. Previous research on p-nitrophenol degradation by *Arthrobacter* sp. found that effective degradation was hampered as the initial p-nitrophenol concentration increased, and no degradation was observed at a concentration of 500 mg/L p-nitrophenol for a period of seven days (Qiu et al., 2009). Nevertheless, no substrate inhibition phenomenon was observed within the tested initial concentration of SMX (5–240 mg/L) when degraded by *Acinetobacter* sp. (Wang et al., 2018). In general, for certain pure or mixed cultures, a proper range of substrate concentration should be indicated for effective degradation of SMZ. Fig. S5c reveals that the TOC mineralization rate varied with the SMZ concentration. When the initial concentration of SMZ was 100 mg/L, it was gradually mineralized and remained stable at 44.0% after 60 h. When the initial SMZ concentration increased to 500 mg/L, a decrease in TOC occurred mainly after 72 h, and with a final TOC removal efficiency of 42.2%. However, when the initial SMZ concentration was 10 mg/L, the TOC reduced slowly within 48 h and reached a steady mineralization rate of 25.1%. The SMZ mineralization rate at 96 h under an initial substrate concentration of 10 mg/L was remarkably lower than that under the initial substrate concentrations of 100 mg/L and 500 mg/L. The possible reason might be that the final SMZ concentrations were 2.9 ± 0.5 mg/L and 3.3 ± 0.6 mg/L corresponding to the initial concentrations of 10 mg/L and 100 mg/L, respectively. This results in almost the same residual TOC concentrations although the initial SMZ concentrations varied greatly. Therefore, the SMZ mineralization rates

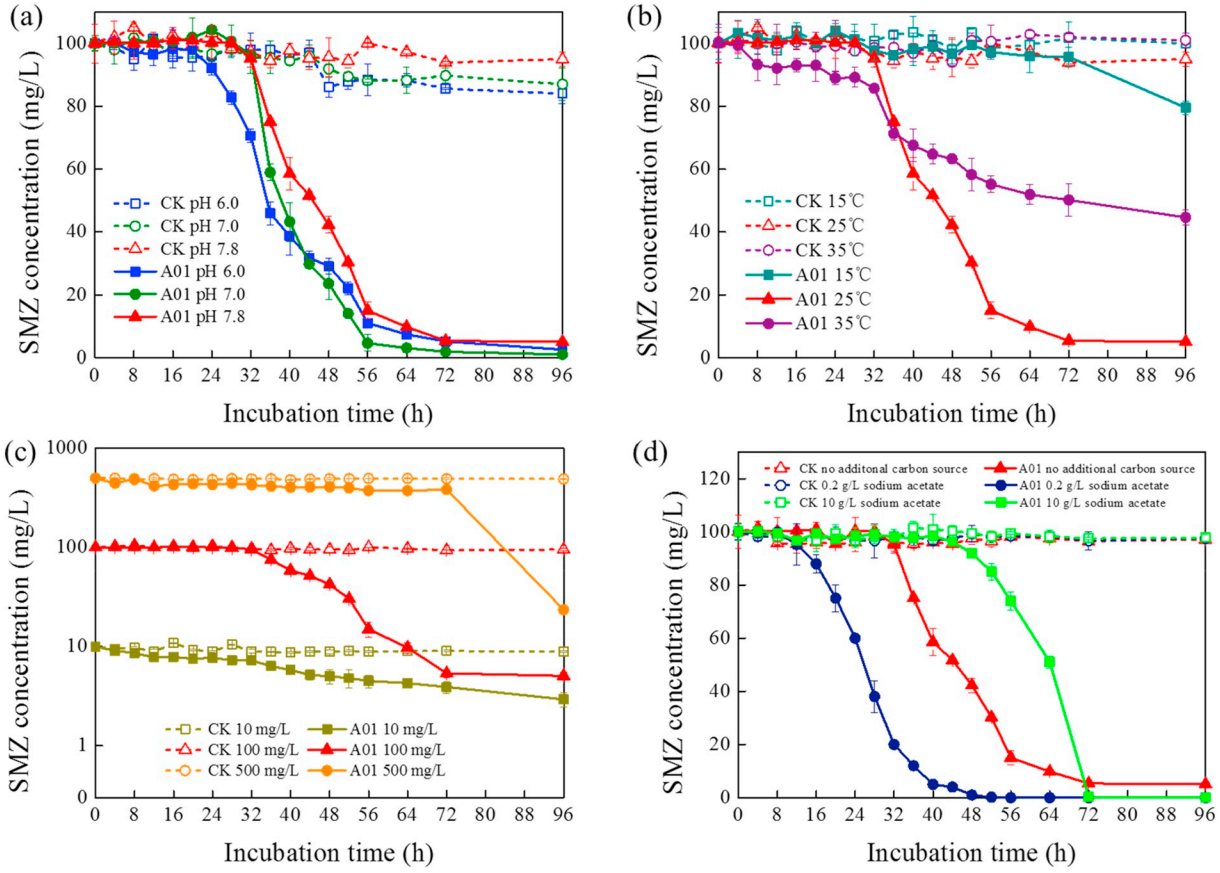

Fig. 3. Effects of (a) pH, (b) temperature, (c) initial SMZ concentration (logarithmic y-axis), and (d) additional carbon source (sodium acetate) on SMZ biodegradation by *Paenarthrobacter* sp. A01. CK represents the control group without cell inoculation.

under different SMZ initial concentrations exhibited remarkably different values.

3.3.4. Effect of additional carbon source on SMZ biodegradation

The addition of sodium acetate had strong impact on the biodegradation of SMZ at 100 mg/L (Fig. 3d). When 0.2 g/L sodium acetate was added as the co-substrate, the biodegradation of SMZ was significantly improved with accelerated bacteria growth (Fig. S6d). This is in accordance with the previous research on SMX biodegradation by *Achromobacter denitrificans* strain PR1, which reported that the SMX removal was augmented considerably by supplementing with 10 mM sodium acetate/succinate (Nguyen et al., 2017). Aside from the accelerated bacteria growth, another possible reason for the enhanced biodegradation of SMZ by dosing additional carbon source might be the occurrence of co-metabolism. Co-metabolism is defined as "the transformation of an organic compound by a microorganism that is unable to use the substrate as a source of energy or of one of its constituent elements" (Alexander, 1994). Co-metabolism has been applied as a promising method for enhanced biodegradation of recalcitrant organic pollutants such as antibiotics, PAHs and halogenated compounds (Haritash and Kaushik, 2009; Dawas-Massalha et al., 2014; Feng et al., 2019). However, it may have inhibitory effect on the biodegradation of contaminants and on microorganism growth if the additional carbon source concentration is greater than the optimal range (Lee et al., 2003). Drillia et al. (2005) reported that the presence of both acetate (300 mg/L) and ammonium prevented SMX biodegradation. In the present study, we observed a similar phenomenon, i.e., a lower degradation rate of SMZ and slower bacteria growth when the added sodium acetate was as high as 10 g/L (Figs. 3d, S6d).

3.4. Kinetic modeling

Various models were studied to evaluate the best model fitting for SMZ biodegradation and co-metabolism with sodium acetate. The modified Gompertz model (Fan et al., 2004) well fit the biodegradation of SMZ by *Paenarthrobacter* sp. A01 with high R^2. The main parameters and their meanings are shown in Table 1. Kinetic characterization of *Paenarthrobacter* sp. A01 utilizing SMZ as the sole carbon source fit the modified Gompertz model with an R^2 of 0.99, which required an adaptation with a lag phase (λ) of 30.1 h and a maximum biodegradation rate (μ_m) of 3.5 mg/ L h^{-1}. When 0.2 g/L sodium acetate was added as the co-substrate, enhanced degradation also fit very well with the modified Gompertz model with a shorter lag phase of 18.1 h and a higher maximum biodegradation rate of 6.1 mg/ L h^{-1}. Deng et al. (2016) studied the co-metabolic biodegradation of sulfadiazine by *Arthrobacter* sp. D2 and *Arthrobacter* sp. D4 and showed that the respective lag phase and maximum biodegradation rate of sulfadiazine degradation by D2 were 7.4 h and 37.1 mg/ L h^{-1}, whereas those by D4 were 0.9 h and 0.2 mg/ L h^{-1}. This is attributed to the differences in the various biodegradation abilities associated with the effectiveness of the enzymes. At an initial concentration of 100 mg/L together with 10 g/L sodium acetate, SMZ biodegradation did not follow the modified Gompertz, zero-order, first-order, second-order, or Richards models which are commonly used for describing substrate utilization processes by microorganisms. Therefore, it is difficult to find a universal model fitting SMZ biodegradation under various conditions. In fact, the real wastewater is highly complex and contains mixed organic carbon sources. Thus, the SMZ biodegradation kinetics is often influenced significantly by many factors, such as the carbon source type, concentration and bioavailability. Nguyen et al. (2018) found that

Table 1
Kinetic parameters of SMZ biodegradation by *Paenarthrobacter* sp. A01.

Carbon source	Initial SMZ concentration	Inoculation amount	Modified Gompertz model				
			Equation	R^2	A (mg/L)	μ_m (mg/L h^{-1})	λ (h)
SMZ	100 mg/L	1.0×10^5 cells/mL	$S = S_0 - A \times exp\left\{-exp\left[\frac{\mu_m e}{A} \times (\lambda - t) + 1\right]\right\}$	0.99	99.1	3.5	30.1
SMZ + 0.2 g/L sodium acetate				0.99	96.3	6.1	18.1

A: biodegradation potential; μ_m: maximum biodegradation rate; λ: lag phase; S_0: calculated initial SMZ concentration.

bioaugmentation of activated sludge with *Achromobacter denitrificans* strain PR1 led to enhanced biodegradation kinetics of SMX when fed with real wastewater as the co-substrate. To evaluate the performance of SMZ biodegradation in a specific environment such as pharmaceutical wastewater or livestock wastewater, further studies are needed to investigate the roles of different carbon sources and their concentrations during the biodegradation process.

3.5. Biodegradation pathways and related functional genes

Identification of SMZ metabolites produced by *Paenarthrobacter* sp. A01 was conducted using HPLC–MS/MS. The total ion chromatograms of compounds appearing after 4 d biodegradation generated from the full-scan mode are shown in Fig. 4a. The peak of SMZ at 7.21 min disappeared when it was removed, and new peaks of possible products arose. The total ion chromatograms of nine putative biodegradation products obtained from the daughter ion scan mode are demonstrated in Figs. S7 and S8. Two of the nine candidate products were confirmed with reference standards, and possible structures of the other seven candidates were proposed.

The highest signal intensity was detected at an RT of 2.63 min in the chromatogram with *m/z* 124 (DP1) (Fig. 4b). The best fitting elemental composition was $C_6H_9N_3$, which corresponds to 2-amino-4, 6-dimethylpyrimidine. This compound was chosen to be the reference standard because previous studies have considered it to be the main biodegradation product of SAs (García-Galán et al., 2011; Sleman et al., 2012; Majewsky et al., 2015). Further confirmation on the RT of the chromatographic peak and the corresponding MS/MS fragments (*m/z* 67, 82, 107) confirmed that DP1 was 2-amino-4, 6-dimethylpyrimidine (Fig. 4c).

DP2, appearing at the RT of 6.63 min, contained a sole ion at *m/z* 215 (Fig. 4d). Its elemental composition was elucidated as $C_{12}H_{14}N_4$, which is related to the loss of the sulfonate group compared with the SMZ molecule. With the confirmation of the standard chemical, DP2 was identified as 2-[N-(4-aminophenyl) amino]-4, 6-dimethylpyrimidine (Fig. 4e). DP2 was also reported in previous studies as the chemical oxidation product and photodegradation product of SAs (García-Galán et al., 2012; Perisa et al., 2013; Zessel et al., 2014; Bai and Acharya, 2016; Fu et al., 2018). It is interesting to note that biodegradation, chemical oxidation, and photodegradation of SAs share the same product, which indicates some general rules might be applied for both biotic and abiotic transformation of SAs. Therefore, further studies need to be conducted to decipher the hidden universal tendency. Such research could also provide a basis for comparing the treatment efficiency and the cost of these different technologies in future application.

Owing to the limited availability of other commercially standards, the structures of the remaining seven biodegradation products detected were inferred from the target *m/z* and their fragment spectra as well as by referring to previous studies (Table S2). DP3 (*m/z* 295) with 16 Da greater than SMZ (*m/z* 279) was identified as the hydroxylated product ($C_{12}H_{14}N_4O_3S$), which is the same as the SMZ degradation under VUV/UV irradiation (Li et al., 2017). DP4 is a new aminosulfonic acid appearing at an RT of 7.39 min. Its peak in the mass spectra was *m/z* 204 which corresponds to (4,6-dimethylpyrimidin-2-yl) sulfamic acid (García-Galán et al., 2012), with the molecular structure of $C_6H_9N_3O_3S$. DP7 was detected at an RT of 7.47 min with *m/z* 159, which was elucidated as $C_{10}H_{10}N_2$ reported from the photodegradation of SMZ (Perisa et al., 2013) or as $C_9H_8N_3$ in SMZ degradation by VUV/UV (Li et al., 2017). However, according to its fragments at *m/z* 92 and 65, the most likely elemental composition is $C_{10}H_{10}N_2$. DP8 presented at an RT of 6.47 min with 15 Da less than DP1 was identified as $C_6H_8N_2$ (Perisa et al., 2013). The structure of DP9 (*m/z* 108) was assumed on the basis of fragment ions at *m/z* 53 and 67. It was formed via a rearrangement occurring in many types of SAs, which have very similar structures (Perisa et al., 2013).

García-Galán et al. (2011) found that N-(4, 6-dimethylpyrimidin-2-yl)-4-(formylamino) benzenesulfonamide with *m/z* of 307 and N-(4, 6-dimethylpyrimidin-2-yl) benzenesulfonamide with *m/z* of 265 are SMZ products degraded by fungus *Trametes versicolor*. However, none of these metabolites were detected in this study. White rot fungi is able to attack a wide range of pollutants owing to its non-specific extracellular enzymes and the intracellular activity of the cytochrome P450 system (Doddapaneni and Yadav, 2004), whereas the degradation process in bacteria relies on specific enzymes coded by the corresponding functional genes. The difference of SMZ biodegradation mechanisms between fungi and bacteria might lead to diverse products as well as different pathways.

DP5 (*m/z* 188) and DP6 (*m/z* 185) are two new products that are first reported in SMZ biodegradation. DP5 was present at an RT of 6.63 min with the elemental composition of $C_6H_9N_3O_2S$ and the possible structure was the loss of a benzene ring and an amino-group. DP6 was observed at an RT of 1.54 min, and its MS/MS fragments were at *m/z* 108 and 78, indicating 4,6-dimethylpyrimidine and a benzene ring, respectively.

Based on the detected products and the formation of DP1 and DP2 in the time series (Fig. 5), three pathways are proposed for the biodegradation of SMZ by A01 (Fig. 6). Strikingly, the concentration of DP2 was very low and it did not accumulate during the entire biodegradation process. Previous research stated that -SO_2- extrusion is a main destruction way of SMZ under simulated solar irradiation (García-Galán et al., 2012). However, it is difficult to assess whether biodegradation pathway I contributed the primary removal of SMZ in the present study. DP1 was detected as a principle product of the bond cleavage between the -SO_2- and -NH- groups. Biodegradation experiments showed that DP1 increased as SMZ decreased and maintained stability when SMZ was removed (Fig. 5). Finally, about 90.7% of SMZ was transformed to DP1. Thus far, the biodegradation mechanism of SMZ remains unclear. $FMNH_2$-dependent monooxygenases were reported to initiate catabolism of SAs in *Microbacterium* sp. strain BR1 subsisting on SAs (Ricken et al., 2017). A cluster of genes encoding sulfonamide monooxygenase (SadA), 4-aminophenol monooxygenase (SadB) and FMN reductase (SadC) enables BR1 and other actinomycetes to inactivate SAs. The alignment of *Paenarthrobacter* sp. A01's ORFs against the NR database showed that the similarities with SadA, SadB and SadC were as high as 96.0%, 100.0%, and 100.0%, respectively, which provides evidence for the assumption of pathway III. SadA catalyzed the initial ipso-hydroxylation, SadB was likely responsible for the downstream pathway oxidizing 4-aminophenol (DP9) to 1,2,4-trihydroxybenzene, and SadC provided the reduced FMN required by both monooxygenases.

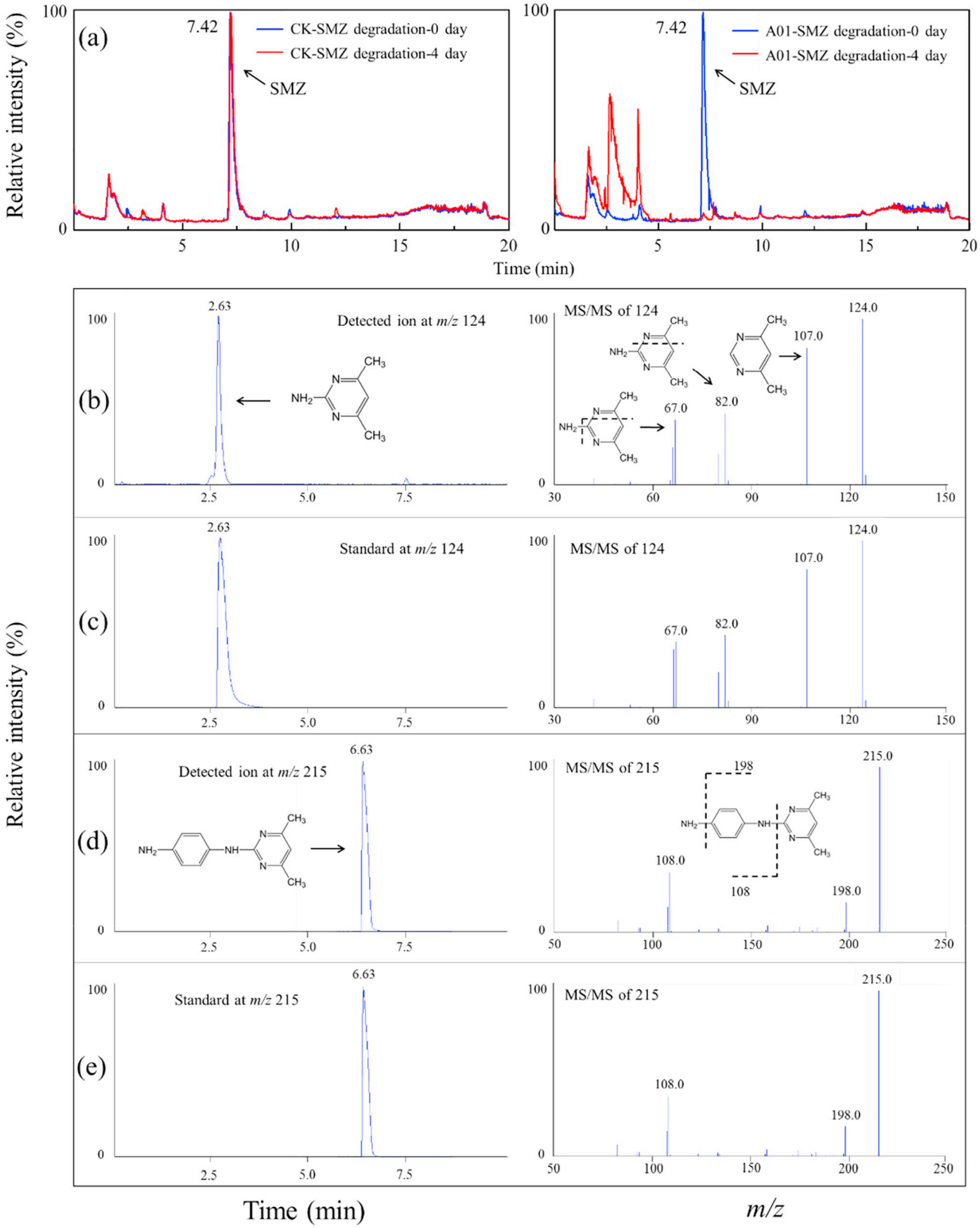

Fig. 4. Identification of the biodegradation products by HPLC–MS/MS. (a) Total ion chromatogram of products generated from full-scan MS mode. CK-SMZ represents the control group without cell inoculation. (b) Chromatogram and MS/MS spectrum of ion at *m/z* 124. (c) Chromatogram and MS/MS spectrum of the standard 2-amino-4, 6-dimethylpyrimidine. (d) Chromatogram and MS/MS spectrum of ion at m/z 215. (e) Chromatogram and MS/MS spectrum of the standard 2-[N-(4-aminophenyl) amino]-4, 6-dimethylpyrimidine.

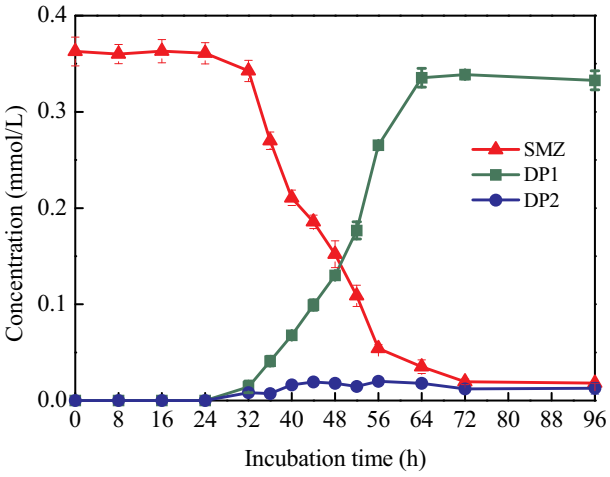

Fig. 5. Biodegradation of SMZ and the coupling formation of DP1 and DP2.

Although the *sadB* gene was found in the genome of A01, the related metabolites of DP9 were not detected in this study possibly because they can be quickly used up by *Paenarthrobacter* sp. A01, resulting in no accumulation of these compounds. Another possible reason is that the concentration of DP9 was below the threshold value so that the reaction was not initiated. It is well documented that no biodegradation process occurs when the substrate concentration is below the threshold value (Pahm and Alexander, 1993; Roch and Alexander, 1997). Insufficient induction of biodegradation genes is often considered as a reason for this phenomenon (Santos et al., 2000; Tros et al., 1996), which could explain the absence of DP9's products in the present study.

4. Conclusions

In this study, a high-efficiency SMZ-degrading strain *Paenarthrobacter* sp. A01, was isolated from activated sludge, and the genomic characterization, kinetics, and pathways of SMZ biodegradation by this strain were analyzed. SMZ with an initial concentration of 100 mg/L was removed almost completely within 72 h at pH 6.0–7.8 and 25 °C. The addition of 0.2 g/L sodium acetate improved the biodegradation efficiency. However, a high initial concentration of 500 mg/L SMZ or 10 g/L sodium acetate as the co-substrate inhibited the biodegradation. *Paenarthrobacter* sp. A01 was able to degrade SMZ into nine biodegradation products via three pathways, among which $C_6H_9N_3O_2S$ and $C_{12}H_{12}N_2$ are two novel products, and 2-amino-4, 6-dimethylpyrimidine was the dominant product with a transformation rate of 90.7%. The sulfur metabolic pathway revealed that *Paenarthrobacter* sp. A01 could not assimilate sulfate and that the -SO_2- moiety of SMZ should be the sole available sulfur source for A01. Additionally, *sad* genes catalyzing SAs biodegradation reactions were identified, and match analysis between the biodegradation genes and the products was also conducted.

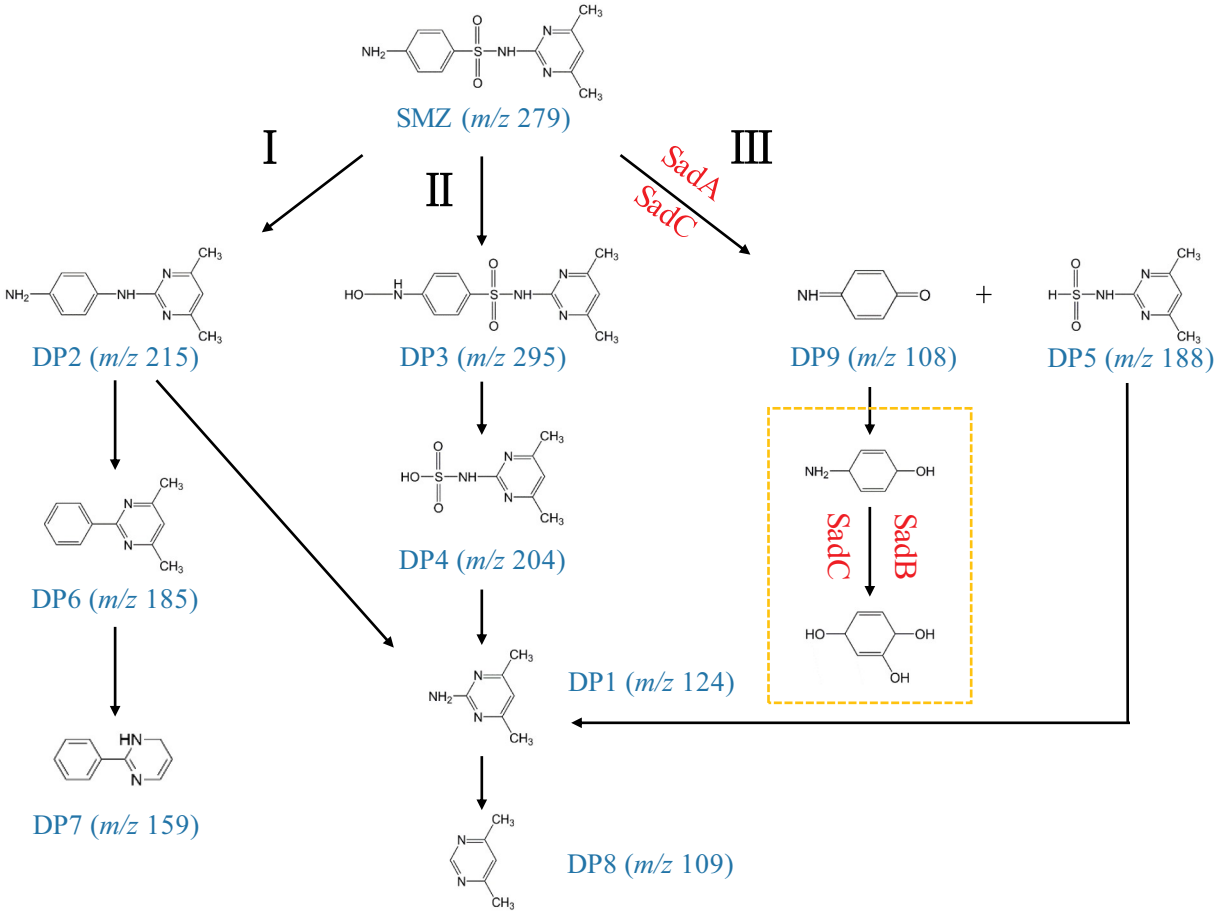

Fig. 6. Proposed SMZ biodegradation pathways and the related functional genes responsible for SMZ biodegradation. The orange rectangle indicates the potential biodegradation products that were not detected by HPLC–MS/MS.

Declaration of Competing Interest

The authors declare that they have no known competing financial interests or personal relationships that could have appeared to influence the work reported in this paper.

Acknowledgements

The authors thank the National Natural Science Foundation of China (No. 21876096), Shenzhen Knowledge Innovation Program-Basic Research Project (JCYJ20170412171918012 and JCYJ20170817161009390), and the Development and Reform Commission of Shenzhen Municipality (Urban Water Recycling and Environment Safety Program) for the financial support on this study.

Appendix A. Supplementary data

Supplementary data to this article can be found online at https://doi.org/10.1016/j.envint.2019.104961.

References

Alexander, M., 1994. Biodegradation and bioremediation. 1994. J. Soils Sediments 4 (3), 209.
Alikhan, N.-F., Petty, N.K., Ben Zakour, N.L., Beatson, S.A., 2011. BLAST Ring Image Generator (BRIG): simple prokaryote genome comparisons. BMC Genomics 12, 402.
Aziz, R.K., Bartels, D., Best, A.A., DeJongh, M., Disz, T., Edwards, R.A., Formsma, K., Gerdes, S., Glass, E.M., Kubal, M., Meyer, F., Olsen, G.J., Olson, R., Osterman, A.L., Overbeek, R.A., McNeil, L.K., Paarmann, D., Paczian, T., Parrello, B., Pusch, G.D., Reich, C., Stevens, R., Vassieva, O., Vonstein, V., Wilke, A., Zagnitko, O., 2008. The RAST server: rapid annotations using subsystems technology. BMC Genomics 9, 75.
Bai, X., Acharya, K., 2016. Removal of trimethoprim, sulfamethoxazole, and triclosan by the green alga *Nannochloris* sp. J. Hazard. Mater. 315, 70–75.
Baran, W., Adamek, E., Ziemianska, J., Sobczak, A., 2011. Effects of the presence of sulfonamides in the environment and their influence on human health. J. Hazard. Mater. 196, 1–15.
Biošić, M., Mitrevski, M., Babić, S., 2017. Environmental behavior of sulfadiazine, sulfamethazine, and their metabolites. Environ. Sci. Pollut. Res. 24 (10), 9802–9812.
Boiangiu, R.S., Andrei, A., Mihasan, M., 2018. Nicotine metabolic genes in *Arthrobacter*: pAO1 vs AK-YN10. Febs Open Bio. 8, 485–486.
Busse, H.J., 2016. Review of the taxonomy of the genus *Arthrobacter*, emendation of the genus *Arthrobacter sensu lato*, proposal to reclassify selected species of the genus *Arthrobacter* in the novel genera *Glutamicibacter* gen. nov., *Paeniglutamicibacter* gen. nov., *Pseudoglutamicibacter* gen. nov., *Paenarthrobacter* gen. nov and *Pseudarthrobacter* gen. nov., and emended description of *Arthrobacter roseus*. Int. J. Syst. Evol. Microbiol. 66, 9–37.
Carvalho, I.T., Santos, L., 2016. Antibiotics in the aquatic environments: a review of the European scenario. Environ. Int. 94, 736–757.
Cheng, M., Zeng, G., Huang, D., Lai, C., Liu, Y., Zhang, C., Wan, J., Hu, L., Zhou, C., Xiong, W., 2018. Efficient degradation of sulfamethazine in simulated and real wastewater at slightly basic pH values using Co-SAM-SCS/H_2O_2 Fenton-like system. Water Res. 138, 7–18.
Dawas-Massalha, A., Gur-Reznik, S., Lerman, S., Sabbah, I., Dosoretz, C.G., 2014. Co-metabolic oxidation of pharmaceutical compounds by a nitrifying bacterial enrichment. Bioresour. Technol. 167, 336–342.
Deng, Y., Mao, Y., Li, B., Yang, C., Zhang, T., 2016. Aerobic degradation of sulfadiazine by *Arthrobacter* spp.: kinetics, pathways, and genomic characterization. Environ. Sci. Technol. 50 (17), 9566–9575.
Deutch, C.E., 2018. L-Proline catabolism by the high G + C Gram-positive bacterium *Paenarthrobacter aurescens* strain TC1. Antonie Van Leeuwenhoek 112 (2), 237–251.
Deutch, C.E., Bui, A.P., Ho, T., 2018. Growth of *Paenarthrobacter aurescens* strain TC1 on atrazine and isopropylamine during osmotic stress. Ann. Microbiol. 68 (9), 569–577.
Doddapaneni, H., Yadav, J.S., 2004. Differential regulation and xenobiotic induction of tandem P450 monooxygenase genes *pc-1* (CYP63A1) and *pc-2* (CYP63A2) in the white-rot fungus *Phanerochaete chrysosporium*. Appl. Microbiol. Biotechnol. 65 (5), 559–565.
Drillia, P., Dokianakis, S.N., Fountoulakis, M.S., Kornaros, M., Stamatelatou, K., Lyberatos, G., 2005. On the occasional biodegradation of pharmaceuticals in the activated sludge process: the example of the antibiotic sulfamethoxazole. J. Hazard. Mater. 122 (3), 259–265.
Fan, Y., Wang, Y., Qian, P.-Y., Gu, J.-D., 2004. Optimization of phthalic acid batch biodegradation and the use of modified Richards model for modelling degradation. Int. Biodeterior. Biodegrad. 53 (1), 57–63.
Feng, N., Yu, J., Xiang, L., Yu, L., Zhao, H., Mo, C., Li, Y., Cai, Q., Wong, M., Li, Q., 2019. Co-metabolic degradation of the antibiotic ciprofloxacin by the enriched bacterial consortium XG and its bacterial community composition. Sci. Total Environ. 665, 41–51.
Fu, W., Li, B., Yang, J., Yi, H., Chai, L., Li, X., 2018. New insights into the chlorination of sulfonamide: smiles-type rearrangement, desulfation, and product toxicity. Chem. Eng. J. 331, 785–793.
Fukahori, S., Ito, M., Fujiwara, T., 2018. Removal mechanism of sulfamethazine and its intermediates from water by a rotating advanced oxidation contactor equipped with TiO_2-high-silica zeolite composite sheets. Environ. Sci. Pollut. Res. Int. 25 (29), 29017–29025.
García-Galán, M.J., Rodríguez-Rodríguez, C.E., Vicent, T., Caminal, G., Díaz-Cruz, M.S., Barceló, D., 2011. Biodegradation of sulfamethazine by *Trametes versicolor*: removal from sewage sludge and identification of intermediate products by UPLC–QqTOF-MS. Sci. Total Environ. 409 (24), 5505–5512.
García-Galán, M.J., Díaz-Cruz, M.S., Barceló, D., 2012. Kinetic studies and characterization of photolytic products of sulfamethazine, sulfapyridine and their acetylated metabolites in water under simulated solar irradiation. Water Res. 46 (3), 711–722.
Garcia-Galan, M.J., Diaz-Cruz, S., Barcelo, D., 2013. Multiresidue trace analysis of sulfonamide antibiotics and their metabolites in soils and sewage sludge by pressurized liquid extraction followed by liquid chromatography-electrospray-quadrupole linear ion trap mass spectrometry. J. Chromatogr. A. 1275, 32–40.
Gui, M., Chen, Q., Ni, J., 2017. Effect of sulfamethoxazole on aerobic denitrification by strain *Pseudomonas stutzeri* PCN-1. Bioresour. Technol. 235, 325–331.
Haritash, A.K., Kaushik, C.P., 2009. Biodegradation aspects of polycyclic aromatic hydrocarbons (PAHs): a review. J. Hazard. Mater. 169, 1–15.
Huang, M., Tian, S., Chen, D., Zhang, W., Wu, J., Chen, L., 2012. Removal of sulfamethazine antibiotics by aerobic sludge and an isolated *Achromobacter* sp. S-3. Environ. Sci. 24 (9), 1594–1599.
Hyatt, D., Chen, G.-L., LoCascio, P.F., Land, M.L., Larimer, F.W., Hauser, L.J., 2010. Prodigal: prokaryotic gene recognition and translation initiation site identification. BMC Bioinf. 11, 119.
Iglesias, A., Nebot, C., Miranda, J.M., Vazquez, B.I., Abuin, C.M.F., Cepeda, A., 2013. Determination of the presence of three antimicrobials in surface water collected from urban and rural areas. Antibiotics 2 (1), 46–57.
Jagdale, G.B., Gordon, R., 1997. Effect of temperature on the activities of glucose-6-phosphate dehydrogenase and hexokinase in entomopathogenic nematodes (nematoda: steinernematidae). Comp. Biochem. Physiol. A Physiol. 118 (4), 1151–1156.
Jiang, B., Li, A., Cui, D., Cai, R., Ma, F., Wang, Y., 2014. Biodegradation and metabolic pathway of sulfamethoxazole by *Pseudomonas psychrophila* HA-4, a newly isolated cold-adapted sulfamethoxazole-degrading bacterium. Appl. Microbiol. Biotechnol. 98 (10), 4671–4681.
Kozich, J.J., Westcott, S.L., Baxter, N.T., Highlander, S.K., Schloss, P.D., 2013. Development of a dual-index sequencing strategy and curation pipeline for analyzing amplicon sequence data on the MiSeq Illumina sequencing platform. Appl. Environ. Microbiol. 79 (17), 5112–5120.
Kumar, S., Stecher, G., Li, M., Knyaz, C., Tamura, K., 2018. Mega X: molecular evolutionary genetics analysis across computing platforms. Mol. Biol. Evol. 35 (6), 1547–1549.
Lee, I., Kim, Y.O., Park, S.-C., Chun, J., 2016. OrthoANI: an improved algorithm and software for calculating average nucleotide identity. Int. J. Syst. Evol. Microbiol. 66, 1100–1103.
Lee, K., Park, J.W., Ahn, I.S., 2003. Effect of additional carbon source on naphthalene biodegradation by *Pseudomonas putida* G7. J. Hazard. Mater. 105 (1–3), 157–167.
Li, D., Luo, R., Liu, C.-M., Leung, C.-M., Ting, H.-F., Sadakane, K., Yamashita, H., Lam, T.-W., 2016. MEGAHIT v1.0: a fast and scalable metagenome assembler driven by advanced methodologies and community practices. Methods 102, 3–11.
Li, M., Wang, C., Yau, M., Bolton, J.R., Qiang, Z., 2017. Sulfamethazine degradation in water by the VUV/UV process: kinetics, mechanism and antibacterial activity determination based on a mini-fluidic VUV/UV photoreaction system. Water Res. 108, 348–355.
Li, W., Shi, Y., Gao, L., Liu, J., Cai, Y., 2013. Occurrence, distribution and potential affecting factors of antibiotics in sewage sludge of wastewater treatment plants in China. Sci. Total Environ. 445-446, 306–313.
Li, Y., Liu, X., Zhang, B., Zhao, Q., Ning, P., Tian, S., 2018. Aquatic photochemistry of sulfamethazine: multivariate effects of main water constituents and mechanisms. Environ. Sci.: Processes Impacts 20 (3), 513–522.
Liu, X., Steele, J.C., Meng, X.Z., 2017. Usage, residue, and human health risk of antibiotics in Chinese aquaculture: a review. Environ. Pollut. 223, 161–169.
Majewsky, M., Glauner, T., Horn, H., 2015. Systematic suspect screening and identification of sulfonamide antibiotic transformation products in the aquatic environment. Anal. Bioanal. Chem. 407 (19), 5707–5717.
Mao, F., Liu, X., Wu, K., Zhou, C., Si, Y., 2018. Biodegradation of sulfonamides by *Shewanella oneidensis* MR-1 and *Shewanella* sp. strain MR-4. Biodegrad. 29 (2), 129–140.
Martin-Laurent, F., Marti, R., Waglechner, N., Wright, G.D., Topp, E., 2014. Draft genome sequence of the sulfonamide antibiotic-degrading *Microbacterium* sp. strain C448. Genome Announc. 2 (1), 011113.
Michael, I., Rizzo, L., McArdell, C.S., Manaia, C.M., Merlin, C., Schwartz, T., Dagot, C., Fatta-Kassinos, D., 2013. Urban wastewater treatment plants as hotspots for the release of antibiotics in the environment: a review. Water Res. 47 (3), 957–995.
Nguyen, P.Y., Carvalho, G., Reis, A.C., Nunes, O.C., Reis, M.A.M., Oehmen, A., 2017. Impact of biogenic substrates on sulfamethoxazole biodegradation kinetics by *Achromobacter denitrificans* strain PR1. Biodegrad. 28 (2–3), 205–217.
Nguyen, P.Y., Carvalho, G., Polesel, F., Torresi, E., Rodrigues, A.M., Rodrigues, J.E., Cardoso, V.V., Benoliel, M.J., Plosz, B.G., Reis, M.A.M., Oehmen, A., 2018. Bioaugmentation of activated sludge with *Achromobacter denitrificans* PR1 for enhancing the biotransformation of sulfamethoxazole and its human conjugates in real wastewater: kinetic tests and modelling. Chem. Eng. J. 352, 79–89.
Pahm, M.A., Alexander, M., 1993. Selecting inocula for the biodegradation of organic compounds at low concentrations. Microb. Ecol. 25 (3), 275–286.
Pan, L.J., Tang, X.D., Li, C.X., Yu, G.W., Wang, Y., 2017. Biodegradation of

sulfamethazine by an isolated thermophile–*Geobacillus* sp. S-07. World J. Microbiol. Biotechnol. 33 (5), 85.
Parks, D.H., Imelfort, M., Skennerton, C.T., Hugenholtz, P., Tyson, G.W., 2015. CheckM: assessing the quality of microbial genomes recovered from isolates, single cells, and metagenomes. Genome Res. 25 (7), 1043–1055.
Perisa, M., Babic, S., Skoric, I., Fromel, T., Knepper, T.P., 2013. Photodegradation of sulfonamides and their N (4)-acetylated metabolites in water by simulated sunlight irradiation: kinetics and identification of photoproducts. Environ. Sci. Pollut. Res. Int. 20 (12), 8934–8946.
Qiu, X., Wu, P., Zhang, H., Li, M., Yan, Z., 2009. Isolation and characterization of *Arthrobacter* sp. HY2 capable of degrading a high concentration of p-nitrophenol. Bioresour. Technol. 100 (21), 5243–5248.
Reis, A.C., Kroll, K., Gomila, M., Kolvenbach, B.A., Corvini, P.F.X., Nunes, O.C., 2017. Complete genome sequence of *Achromobacter denitrificans* PR1. Genome Announc. 5 (31), 00762-17.
Reis, P.J.M., Reis, A.C., Ricken, B., Kolvenbach, B.A., Manaia, C.M., Corvini, P.F.X., Nunes, O.C., 2014. Biodegradation of sulfamethoxazole and other sulfonamides by *Achromobacter denitrificans* PR1. J. Hazard. Mater. 280, 741–749.
Ricken, B., Kolvenbach, B.A., Bergesch, C., Benndorf, D., Kroll, K., Strnad, H., Vlček, Č., Adaixo, R., Hammes, F., Shahgaldian, P., Schäffer, A., Kohler, H.-P.E., Corvini, P.F.X., 2017. $FMNH_2$-dependent monooxygenases initiate catabolism of sulfonamides in *Microbacterium* sp. strain BR1 subsisting on sulfonamide antibiotics. Sci. Rep. 7 (1), 15783.
Roch, F., Alexander, M., 1997. Inability of bacteria to degrade low concentrations of toluene in water. Environ. Toxicol. Chem. 16 (7), 1377–1383.
Sangwan, N., Verma, H., Kumar, R., Negi, V., Lax, S., Khurana, P., Negi, V., Lax, S., Khurana, P., Khurana, J.P., Gilbert, J.A., Lal, R., 2014. Reconstructing an ancestral genotype of two hexachlorocyclohexane-degrading *Sphingobium* species using metagenomic sequence data. ISME J. 8 (2), 398–408.
Santos, P.M., Blatny, J.M., Di Bartolo, I., Valla, S., Zennaro, E., 2000. Physiological analysis of the expression of the styrene degradation gene cluster in *Pseudomonas fluorescens* ST. Appl. Environ. Microbiol. 66 (4), 1305–1310.
Sleman, F., Mahmoud, W.M.M., Schubert, R., Kümmerer, K., 2012. Photodegradation, photocatalytic, and aerobic biodegradation of sulfisomidine and identification of transformation products by LC-UV-MS/MS. Clean: Soil, Air, Water 40 (11), 1244–1249.
Spielmeyer, A., Hoper, H., Hamscher, G., 2017. Long-term monitoring of sulfonamide leaching from manure amended soil into groundwater. Chemosphere 177, 232–238.
Tibbett, M., Sanders, F.E., Cairney, J.W.G., 1998. The effect of temperature and inorganic phosphorus supply on growth and acid phosphatase production in arctic and temperate strains of ectomycorrhizal *Hebeloma* spp. in axenic culture. Mycol. Res. 102 (2), 129–135.
Tros, M.E., Bosma, T., Schraa, G., Zehnder, A., 1996. Measurement of minimum substrate concentration (Smin) in a recycling fermentor and its prediction from the kinetic parameters of *Pseudomonas* strain B13 from batch and chemostat cultures. Appl. Environ. Microbiol. 62 (10), 3655–3661.
Varghese, N.J., Mukherjee, S., Ivanova, N., Konstantinidis, K.T., Mavrommatis, K., Kyrpides, N.C., Pati, A., 2015. Microbial species delineation using whole genome sequences. Nucleic Acids Res. 43 (14), 6761–6771.
Wang, J., Wang, S., 2018. Microbial degradation of sulfamethoxazole in the environment. Appl. Microbiol. Biotechnol. 102 (8), 3573–3582.
Wang, L., Wu, Y.C., Zheng, Y., Liu, L.D., Zhao, F., 2015b. Efficient degradation of sulfamethoxazole and the response of microbial communities in microbial fuel cells. RSC Adv. 5, 56430–56437.
Wang, Q., Garrity, G.M., Tiedje, J.M., Cole, J.R., 2007. Naive Bayesian classifier for rapid assignment of rRNA sequences into the new bacterial taxonomy. Appl. Environ. Microbiol. 73 (16), 5261–5267.
Wang, S., Wang, J., 2017. Biodegradation and metabolic pathway of sulfamethoxazole by a novel strain *Acinetobacter* sp. Appl. Microbiol. Biotechnol. 102 (1), 425–432.
Wang, S., Li, S., Zhang, X., Wei, Y., Zhang, M., Zhang, J., 2015a. Analysis of sulfonamids and their metabolites in drinking water by high performance liquid chromatography tandem mass spectrometry. J. Hyg. Res. 44 (4), 652–657.
Wang, S., Hu, Y., Wang, J., 2018. Biodegradation of typical pharmaceutical compounds by a novel strain *Acinetobacter* sp. J. Environ. Manag. 217, 240–246.
Wu, Y., Ke, X., Hernandez, M., Wang, B., Dumont, M.G., Jia, Z., Conrad, R., 2013. Autotrophic growth of bacterial and archaeal ammonia oxidizers in freshwater sediment microcosms incubated at different temperatures. Appl. Environ. Microbiol. 79 (9), 3076–3084.
Yang, C., Hsiao, W., Chang, B., 2016. Biodegradation of sulfonamide antibiotics in sludge. Chemosphere 150, 559–565.
Yang, Z., Jiang, W., Wang, X., Cheng, T., Zhang, D., Wang, H., Qiu, J., Cao, L., Wang, X., Hong, Q., 2018. An amidase gene, *ipaH*, is responsible for the initial step in the iprodione degradation pathway of *Paenarthrobacter* sp strain YJN-5. Appl. Environ. Microbiol. 84 (19), 01150-18.
Yin, X., Qiang, Z., Ben, W., Pan, X., Nie, Y., 2014. Biodegradation of sulfamethazine by activated sludge: lab-scale study. J. Environ. Eng. 140 (7), 04014024.
Zarfl, C., Matthies, M., Klasmeier, J., 2008. A mechanistical model for the uptake of sulfonamides by bacteria. Chemosphere 70 (5), 753–760.
Zessel, K., Mohring, S., Hamscher, G., Kietzmann, M., Stahl, J., 2014. Biocompatibility and antibacterial activity of photolytic products of sulfonamides. Chemosphere 100, 167–174.
Zhang, G., Li, B., Liu, J., Luan, M., Yue, L., Jiang, X., Yu, K., Guan, Y., 2018. The bacterial community significantly promotes cast iron corrosion in reclaimed wastewater distribution systems. Microbiome 6 (1), 222.
Zhao, R.X., Feng, J., Fu, W.J., Li, X.Y., Li, B., 2019. Deciphering of microbial community and antibiotic resistance genes in activated sludge reactors under high selective pressure of different antibiotics. Water Res. 151 (15), 388–402.